

UNEXPECTED PRESENCE OF SOLUTE-FREE ZONES AT METAL-WATER INTERFACES

*B. Chai, A. G. Mahtani, G. H. Pollack**

Department of Bioengineering, Box 355061, University of Washington,
Seattle, WA 98195

Abstract: Solute-free zones, termed “exclusion zones” are routinely seen next to hydrophilic surfaces in aqueous solution. Here we report similar zones next to various metals. The largest, approximately 200 μm in width, was found adjacent to zinc. Other reactive metals, including aluminum, tin, lead, and tungsten exhibited distinct but smaller exclusion zones, while precious metals such as platinum and gold did not produce any. Electrical potential measurements showed positive potentials within the exclusion zones, while pH measurements revealed an abundance of OH groups in the aqueous regions beyond the exclusion zones. A correspondence was found between exclusion-zone size and the respective metal’s position within the galvanic series. The presence of these interfacial exclusion zones is unexpected, and may shed new light on electrochemical processes taking place at metal interfaces.

Keywords: metals, aqueous solution, oxidation, metal-water interfaces, charge separation, exclusion zones.

1. INTRODUCTION

The interaction of water with metal surfaces is of interest not only from a fundamental surface-science perspective, but also in the context of corrosion and catalysis. The first few water layers adjacent to metal surfaces have been widely investigated [1–5], but many questions remain open [6–7]. Most studies of wetted surfaces have focused on the first few molecular layers of water, whose arrangement appears to be similar to molecules in the densest layers of ice⁴. Molecular dynamics simulations found stable ordering in the first layers in strongly interacting metals, but less stability next to noble metals [6].

Interfacial water has also been studied next to various non-metal hydrophilic surfaces [8]. These studies have revealed large solute-exclusion zones (EZs) extending up to several hundred micrometers from the surface [8–12]. The surfaces have included various gels, polymers, monolayers, and biological specimens. The zones of interfacial water are physically distinct, less mobile, and more ordered than surrounding bulk water. The presence of interfacial exclusion zones adjacent to these surfaces raises the question of whether EZs might also exist alongside other solid surfaces, such as those of metals.

In this study, we find positively charged exclusion zones of substantial size next to several reactive metal surfaces. Nobler metals such as platinum and gold did not produce such zones. The presence of these zones may bear directly on the understanding of metal-surface electrochemical processes.

2. MATERIALS AND METHODS

Sample preparation. The metal foils used in these experiments included the following: zinc (0.25 mm thick), aluminum (0.25 mm), tin (0.5 mm), lead (0.127 mm), tungsten (0.127 mm), copper (0.25 mm), platinum (0.125 mm) and gold (0.125 mm). All metals were purchased from Sigma-Aldrich and had 99.99% purity. The metal foils were cut to the dimensions of 25 mm x 3 mm before use. If the metal sample was not freshly purchased, then before each use the surfaces were cleaned. For the active metals, Zn, W, Pb, Sn and Al, any obvious surface-oxidation layer was removed with fine sand paper (grit size 400) followed by a deionized water rinse. For noble metals, Pt and Au, the surface was merely rinsed with deionized water, as oxidation layers were not obviously present. All experiments were carried out at room temperature, 21 - 22°C.

The water used in all experiments was obtained from a NANOpure Diamond ultrapure water

*Corresponding author: ghp@u.washington.edu

system. The purity of water from this system is certified by resistivity values up to 18.2 M Ω -cm, which exceeds ASTM, CAP, and NCCLS type-I water requirements. In addition, the deionized water was passed through a 0.2 μ m hollow-fiber filter, ensuring bacteria- and particle-free water. After filtration, this water had a pH of 5.5 - 6.

To quantify the size of the exclusion zone, various functionalized microspheres were used, all 1- μ m diameter. These microspheres included carboxylate (2.65% solid-latex, Polysciences Inc.), polystyrene (2.65% solid-latex, Polysciences Inc.), amino (2.66% solid-latex, Polysciences Inc.), amidine (4.1% solid-latex, Invitrogen) and 488-nm-excitation fluorescent amine-modified microspheres (2% solid, yellow-green fluorescence, Invitrogen). The volume fraction of fluorescent microspheres to

water was 1:250, and for all other microspheres it was 1:400. For routine microscopic and oxidation experiments, a 2.5 mL carboxylate suspension was used.

Experimental Chamber. The chamber used for electrical potential measurements, as well as for inverted and confocal microscopic observations, is shown in Figure 1. It consisted of a 1-mm thick glass slide, secured to the bottom of 12-mm thick polycarbonate plastic block (75 mm \times 42 mm) with a 25 \times 18 mm rectangular cavity in the center. A clamp system of two thumb-screws ensured perpendicular mounting of the metal foil. A 45° access bevel was built in on the opposite side of the thumb screws, allowing for easier mobility of the electrode probe for potential measurements.

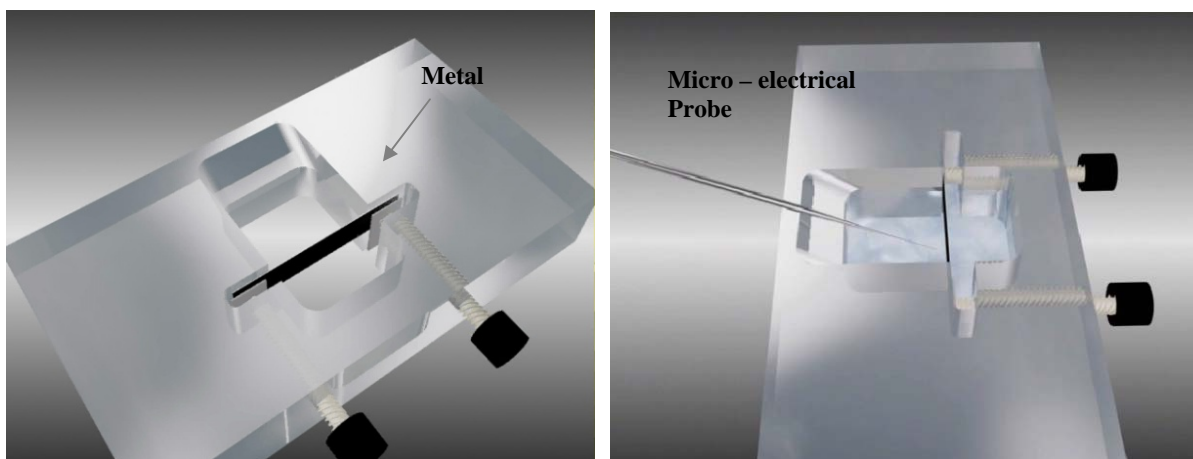


Figure 1. Chamber used for microscope observations and electrical potential measurements.

Microscope Observations. A Zeiss Axiovert 35 inverted microscope was used for standard microscopic observations. A high-resolution single chip color digital camera (CFW-1310C, Scion Corporation), well suited for low-light color video microscopy, was used for capturing images. The chip has a pixel resolution of 1360 \times 1024 and a dynamic range of 10 bits. The CCD sensor employs the widely used Bayer color-filter arrangement. All image processing was done via ImageJ software.

Confocal Microscope. A Zeiss LSM 510 confocal microscope (UW NanoTech User Facility) was used to obtain 3D images, for detailed analysis of the EZ next to zinc. The system is equipped with an inverted Axiovert 200 motorized microscope stage and has Argon laser excitations at 458 nm, 477 nm and 488 nm. For the 3D image scans, the zinc sam-

ple (12 mm \times 0.25 mm \times 1 mm) was scanned at 2- μ m intervals along the Z-axis.

Potential Measurements. To make the electrical potential measurements, reference and probe electrodes were used. The probe electrodes were standard tapered glass microelectrodes. Thin-walled, single-barrel borosilicate capillary tubes (O.D. = 1.2 mm, Model TW150F-6, World Precision Instruments) were single-pulled using a standard electrode puller (P-87, Sutter Instruments). The pulled electrodes were immersed in a 3M KCl solution with the tip facing upward, causing the solution to climb to the tip via capillary action, and allowing the electrode tip to be bubble free. The microelectrode was then back-filled using a flexible long syringe tip. The resistance was measured to be \sim 10 M Ω . The electrodes were connected to an Electro 705 battery-

operated, low noise, wide-band electrometer preamplifier (World Precision Instruments Inc.), designed for intracellular voltage measurement. A coated glass Micro Dri-Ref reference electrode (World Precision Instruments Inc.), 450 μm in diameter and 8 cm in length, was positioned at a distance of 2 cm from the metal surface in the bulk water, while the probe electrode, set at an angle of 45° to the horizon, was advanced by a motor at a speed of 10 $\mu\text{m/s}$. A stereo microscope and CCD camera were used to monitor and confirm the electrode-tip position to avoid tip breakage during movement and advancement.

pH Measurements. Two types of pH measurements were made in bulk regions beyond the EZ: one used a pH probe to track the time course of pH changes at fixed locations; the other used a pH indicator dye for visualization of pH distribution. For both measurements, a rectangular glass chamber 25-mm deep was built with base dimensions of 35 mm \times 6 mm. The chamber's floor was fully covered with the metal to be tested and eight milliliters of deionized water was poured into the chamber.

To determine local hydrogen-ion concentration, a pH probe (Orion 8272BN PerpHect® Ross® Sure-Flow pH Electrode, Thermo Scientific) was connected to a standard pH meter (Orion 350 Perp-

Hect® Advanced Benchtop pH Meter, Thermo Scientific). The pH probe was lowered into the aqueous solution-filled chamber 5 mm above the metal surface.

For the pH indicator dye experiments, a Riedel-de Haën® Universal indicator (pH 3.0-10.0, Sigma Aldrich) was diluted as per the manufacturer's recommendation and poured slowly into the chamber. The local pH change was recorded using a CCD camera and ImageJ.

3. RESULTS

Microscopic observations

1. Basic observations

Figure 2 shows representative images of solute-free zones adjacent to various metal samples. Although exclusion zones immediately formed next to these metals, images were captured after 30 minutes to ensure that the EZ size had reasonably stabilized. The time course of EZ growth depended on the type of metal, and is described in more detail in section 1.3. Panels *a - e* show EZs beyond the reactive metal surfaces, while panel *f* is a representative image of a platinum sample, which does not generate an EZ under the conditions studied.

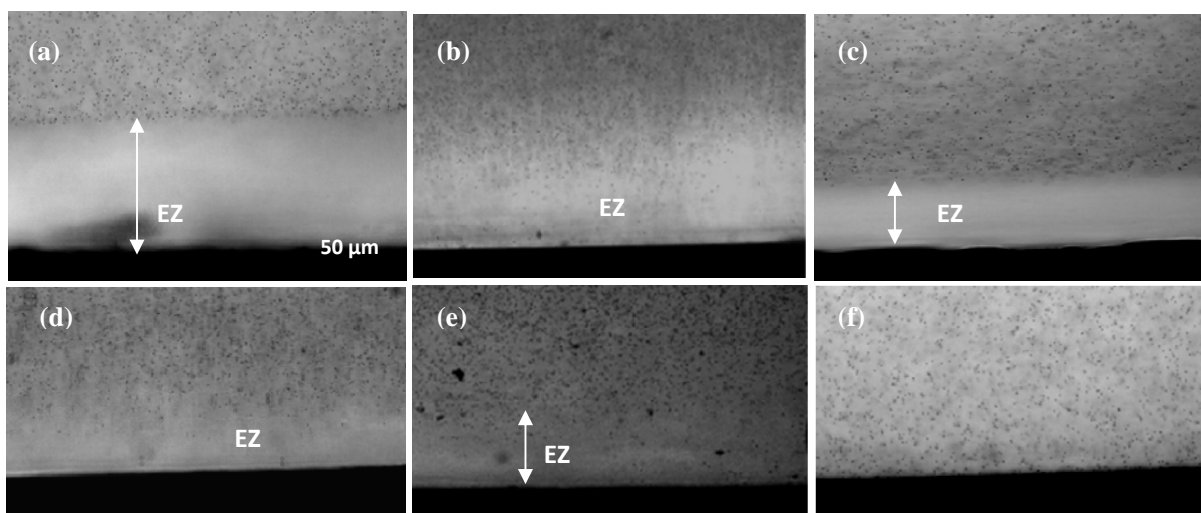


Figure 2. Microsphere-free zones adjacent to surfaces of different metals: (a) zinc; (b) aluminum; (c) lead; (d) tungsten, (e) tin, and (f) platinum. All images obtained 30 min following exposure to microsphere suspension.

2. EZ Coverage

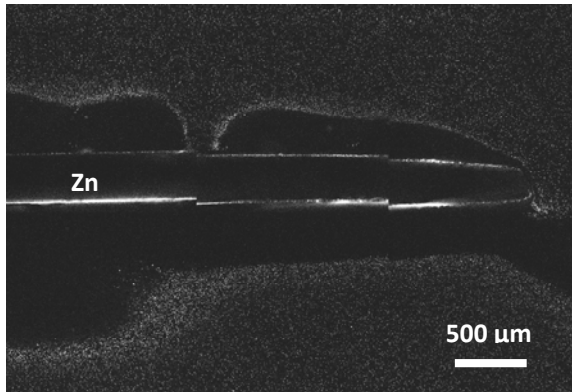


Figure 3. Confocal microscope image of an exclusion zone near zinc. Note the continuous EZ on one side of the zinc (below) and the pockets of exclusion on the other side (above).

Coverage Next to Zinc. Figure 3 shows a representative 2D confocal image of an EZ adjacent to a zinc surface, obtained using fluorescent microspheres. In some regions, the EZ covered the full breadth of the zinc surface, while other regions showed large “pocket” zones of exclusion, where microspheres accumulated near the metal surface between pockets.

Reconstructed 3-D confocal microscope images seen from different view angles are shown in Figure 4. The red dashed lines in panel *a* show the

outline of the zinc sample. Axes are shown in green on all panels. The figures show the fluorescent microspheres and microsphere-free zones from different perspectives. Most focal planes showed fairly uniform EZs $\sim 250\text{-}\mu\text{m}$ wide. The top view, Figure 4(c), shows no EZ near the top focal layers at one end, but a uniform EZ ($\sim 200\ \mu\text{m}$) at the other end. The results show substantial but incomplete coverage. In general, we found that fresher samples tended to show more complete coverage than those that had been used and cleaned, although this feature was not studied in detail.

EZ Coverage Next to Other Reactive Metals.

Microscopic observations of the interaction between colloidal microsphere suspension and interfaces were carried out near other reactive metal surfaces besides zinc. The results are summarized in Table 1. The fractional coverage was obtained by calculating the ratio of the length of EZ surface to the length of the metal piece at every focal plane (X-Y plane) explored, and then averaging data from all planes along the Z-direction. From Table 1, it is apparent that the EZ width was largest next to zinc, with aluminum, lead, tin, and tungsten following in order of size. The largest fractional coverage was also found next to zinc, with only relatively small regions devoid of any EZ. The gold and platinum were not included in the table since they showed no EZ under the measurement conditions.

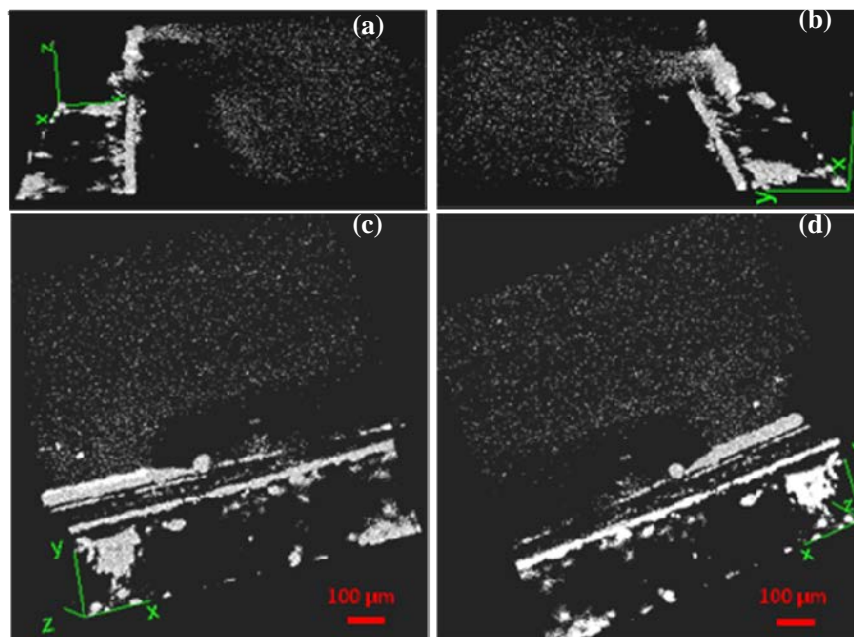


Figure 4. Confocal 3D images of EZ distribution near zinc reconstructed from different view angles: (a) left side view (b) right side view (c) top view (d) bottom view.

Table 1. EZ width and fractional coverage, measured with carboxylate microspheres ($n = 4$)

	Zinc	Aluminum	Lead	Tin	Tungsten
Average EZ size (μm)	220	105	95	90	72
Standard deviation \pm (μm)	46.5	25.2	21.5	19.0	20.1
Average fractional coverage	93%	42%	55%	40%	58%
Standard deviation \pm (%)	5%	8%	10%	7%	12%

3. Time Course of EZ Growth

The growth rate of the solute-free zones differed among the various metals. Figure 5 shows EZ growth as a function of time near zinc. It can be seen that the EZ grew to a maximum of approximately 350 μm after 20 minutes and then stabilized at approximately 220 μm by 40 minutes.

The aluminum EZ grew more slowly. In the first several minutes it grew to only 10 μm and increased to 100 μm by approximately 20 minutes. In the case of tungsten, an EZ was not visible at all until 20 minutes, and then grew steadily to 70 μm at 60 minutes. Lead behaved similarly to zinc, achieving a maximum EZ size of 200 μm at 15 minutes, and subsequently declining to 100 μm at 40 minutes. Thus EZ-growth dynamics depended on the particular metal.

4. Effect of microsphere charge

To examine whether near-metal EZ formation is an intrinsic feature of metal-water interaction, independent of microsphere charge, different types of functionalized microsphere were used: polystyrene (negatively charged); amino (slightly negative at $\text{pH} > 5$; experimental pH 5.25); and amidine (positive at $\text{pH} < 8$, experimental pH 5.68). The experiments were conducted adjacent to zinc, under conditions similar to those of previous experiments with carboxylate microspheres. Average EZ widths, respectively, for the three microsphere types were $267 \pm 35 \mu\text{m}$, $200 \pm 110 \mu\text{m}$, and $295 \pm 58 \mu\text{m}$. With standard carboxylate microspheres, EZ width was 220 μm . Hence microsphere charge had a relatively minor effect on the results.

Next to precious metals, however, the results were somewhat less consistent. Carboxylate, amino and polystyrene microspheres failed to reveal an

exclusion zone in any of those metals. However, amidine microspheres did sometimes reveal either an exclusion zone or a low-concentration zone. In the case of gold, microsphere exclusion occurred in 80% of the amidine experiments, the remaining 20% displaying no exclusion. When the microspheres were excluded, half of the runs showed immediate exclusion, with subsequent slow return toward zero (time constant ~ 30 min), while the other half showed only a zone of low concentration that appeared within ~ 10 min and persisted for ~ 100 minutes before returning to the initial concentration. In the case of platinum, a zone of low microsphere concentration was again seen. It reached a maximum size of $\sim 270 \mu\text{m}$ at 40 minutes, then gradually decreased to $\sim 200 \mu\text{m}$ and remained stable at that value for two hours.

Electrical potential measurements

The electrical potential distributions were measured in the exclusion zones next to zinc and aluminum. Results are shown in Figures 6. From Figure 6(a), it can be seen that as the probe advanced closer to the zinc surface, positive potentials began to register, the magnitude increasing with increasing proximity to the surface. At the surface, the potential was approximately +200 mV.

Next to aluminum, results were less consistent (Fig. 6b). In approximately half the trials ($n = 8$), the results were fairly similar to zinc, although the gradient was significantly steeper with the near-surface potential reaching +120 mV. In the other half of trials, made in different regions of the same samples, the results showed near-zero values from beyond the EZ all the way to the surface. Since EZ coverage of the surface was approximately 50%, we assume that these differences are reflections of whether the probe penetrated into the EZ or into regions lacking an EZ.

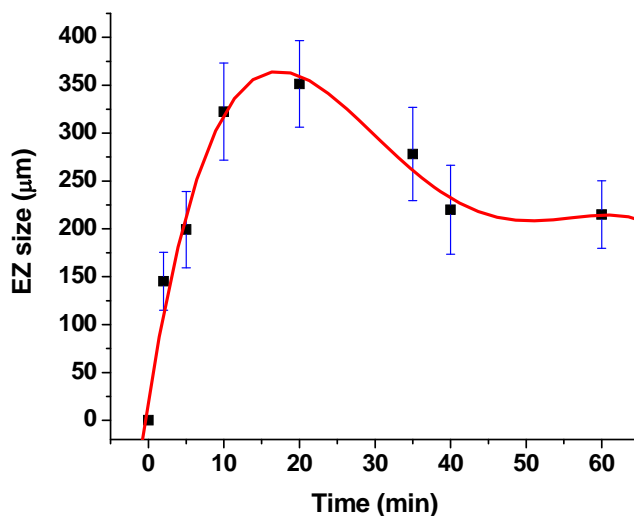


Figure 5. Time course of zinc EZ width, measured using carboxylate microspheres. Standard deviations are indicated by bars. Data points were fitted with a polynomial distribution.

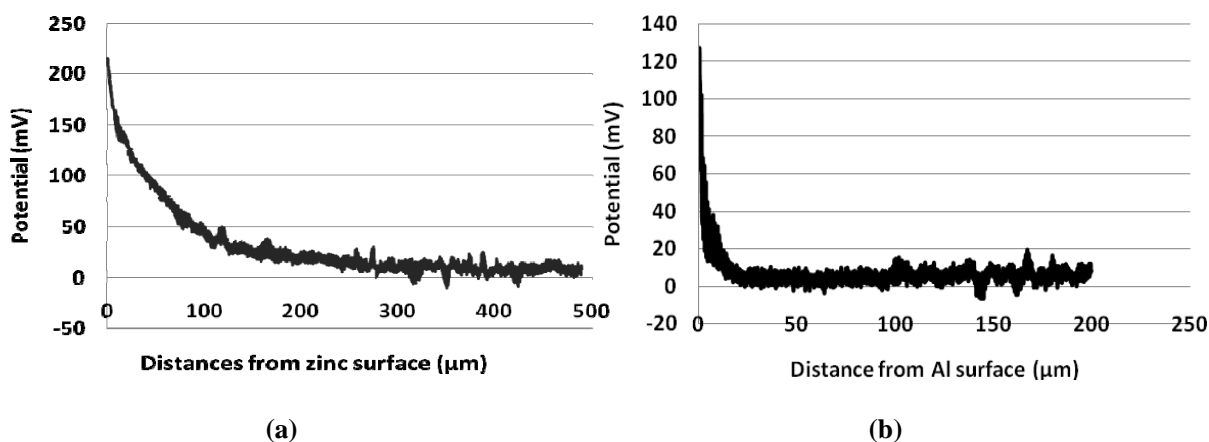


Figure 6. Potential distribution near surfaces of zinc (a) and aluminum (b). In both panels the results are averages of three measurements. In panel b, the average was obtained from three results that showed similar patterns, which occurred in approximately half of runs. The other half were qualitatively different.

pH measurements

To complement the electrical potential measurements, a pH indicator dye was used for visualizing the pH distribution. Representative results for zinc and aluminum are shown in Figure 7. Initially, the entire chamber showed a uniform orange color, corresponding to a pH of approximately 5. By 10 minutes, a yellowish color began to appear in the vicinity of the zinc, becoming greener with time. Eventually the entire volume passed from yellow to green, the latter indicating a pH value near 8. The alkalinity appeared to arise from near the zinc surface, as stre-

aks of green could be seen emanating from the metal at 30, 40 and 60 minutes. The pH changes near the aluminum (figure 7b) were similar, but less pronounced. There, the pH of the water shifted approximately from 5 to 7 within a period of 60 min.

Figure 8 shows a close up view of the zinc surface, taken at 20 minutes after the pH-indicator solution had been poured into the chamber. Regions close to the zinc surface show less intense dye color (lines), indicating exclusion of the pH dye. Regions beyond these clearer zones are greenish or purplish in color, indicating high pH value.

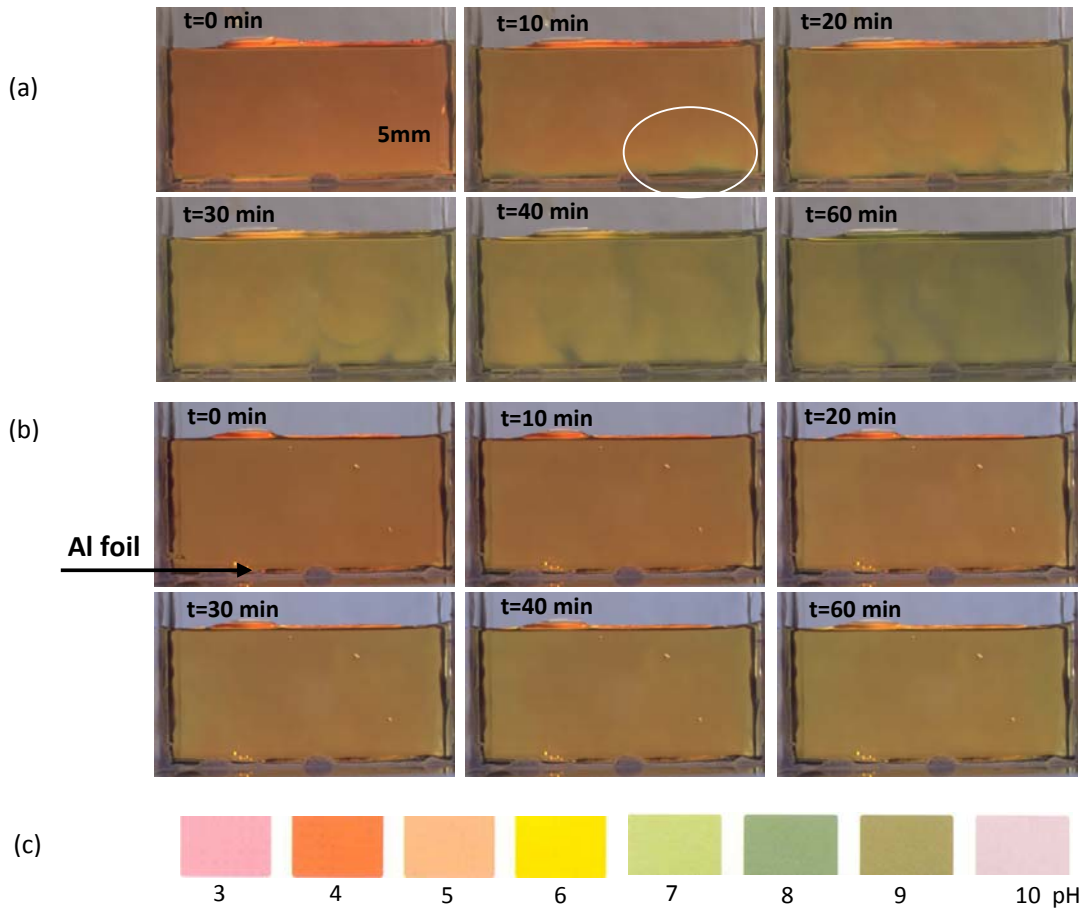


Figure 7. Time course of pH changes when a zinc (a) or aluminum (b) sheet covered the bottom of the glass chamber containing pH indicator; (c) pH color scale for universal pH indicator.

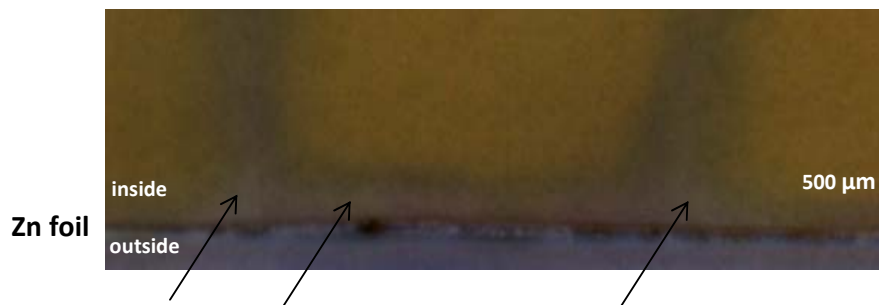


Figure 8. High-magnification view of pH dye near a zinc surface. The zinc foil covers the entire floor of the chamber, as indicated by left arrow. Oblique arrows show lighter regions, indicating exclusion of dye.

To validate the pH-dye results, a pH probe was positioned 5 mm beyond the metal surface, and pH values were recorded as a function of time (Figure 9). These results correspond well with the pH-dye measurements in the following respects: (1) initially, pH values increased with time; (2) pH changes were

larger with zinc than with aluminum; (3) in the case of zinc, both methods show a pH swing on the order of three to four pH units. In the case of zinc, pH increased to a maximum, followed by a slow decline. The decline was probably small enough to have gone undetected in the dye experiments.

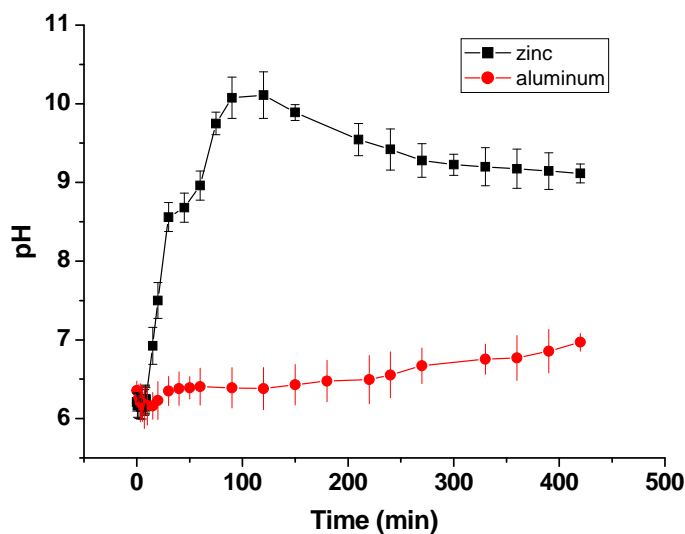


Figure 9. pH changes measured 5 mm from metal surface, obtained using a pH-sensitive probe ($n=4$).

EZ and Oxidation

Because metals often oxidize in the presence of water, we considered the possible relationship between oxidation and exclusion-zone formation. Thus, completely fresh, presumably unoxidized samples of zinc with the same dimensions as the samples used in microscopic observations were tested.

Figure 10 shows a time series of EZ buildup near the zinc surface. Panel (a) shows an image obtained very shortly after the microsphere solution had been injected into the chamber. Pocket EZs formed initially, as outlined in red. By about 1.5 minutes the EZ became uniform throughout the length of the sample without increasing in size (b). Over the next 40 minutes the EZ remained uniform, first increasing and then slightly decreasing in size (c, d). At approximately 40 minutes, pocket exclusion zones often began to appear, increasing progressively in number. After the hour-long experiment, the surface was generally covered with a thin white film of oxidation. When examined microscopically, the film appeared to consist of thin, mostly vertically oriented strips approximately 50–100 μm wide and roughly 600 μm apart (Fig. 11).

Interestingly, the oxidation pattern corresponded well to the EZ distribution pattern. In situations in which the exclusion zone had remained uniform throughout the experiment (e.g., Figure 10), oxidation strips were absent. In cases in which pocket exclusion zones developed, oxidation strips were observed. The pocket exclusion zones typically

extended along a more-or-less vertical axis, as shown in Figure 12. This vertical feature was similar to the oxidation lines. Hence, there was reasonable correlation between the exclusion-zone pattern and the oxidation pattern: oxidation occurred in places where there were gaps between exclusion zones.

4. DISCUSSION

Exclusion Zone Next to Metals

Previous results from this laboratory have confirmed the presence of extensive interfacial exclusion zones in water adjacent to various hydrophilic surfaces [9–16]. Projecting out to a maximum of hundreds of micrometers from the surface, these zones have different physical and chemical characteristics than bulk water [9,12]. Their most obvious feature is the exclusion of particles and solutes.

Here we found that exclusion zones also exist next to various metal surfaces. Among them, zinc showed the widest EZs as well as the highest surface coverage. Other reactive metals showed relatively smaller zones and less coverage. Noble metals such as platinum and gold did not generally show obvious EZs, although we did notice that gold could exhibit an EZ or low-concentration zone when exposed to an amidine microsphere suspension, and that platinum could show low concentration zones as well under similar conditions. At this stage we are unable to account for these exceptions.

Also observed was that the time courses of EZ development depended on time. Typically, some tens of minutes were required for full development,

and there was commonly some diminution of size following that development.

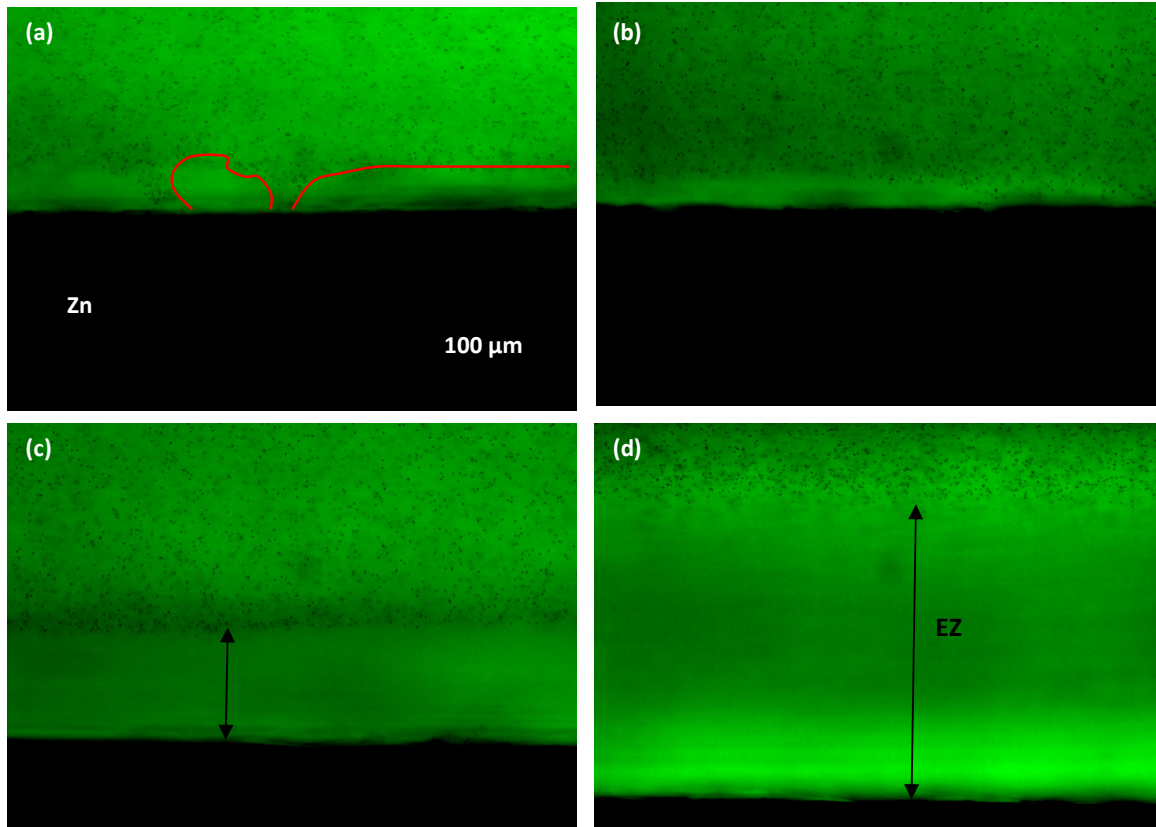


Figure 10. EZ development adjacent to a fresh zinc sample following injection of carboxylate-microsphere suspension. (a) 1.5 seconds; (b) 1.5 minutes; (c) 2.5 minutes; (d) 21 minutes. Representative of four experiments.



Figure 11. Comparison of fresh zinc, before (a) and after (b) immersing into microsphere suspension for 1 hour.

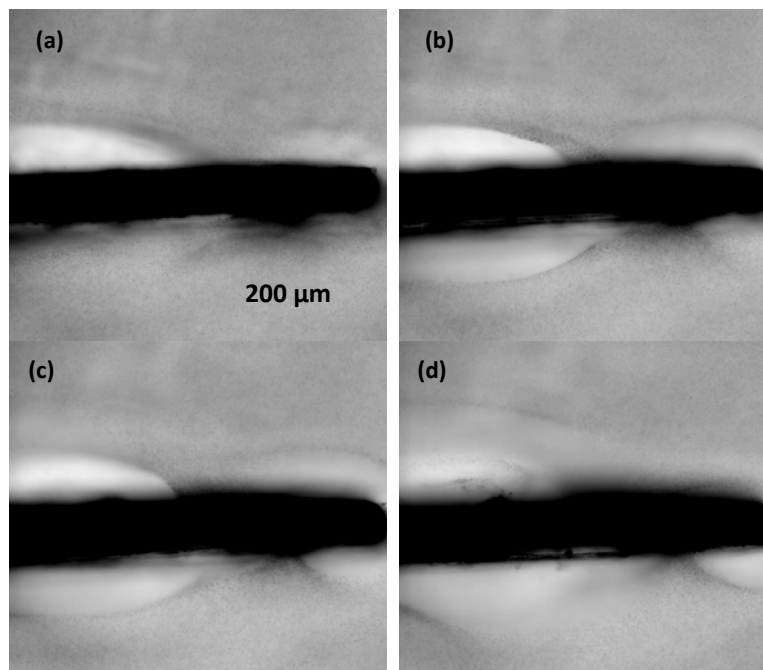


Figure 12. Exclusion zones at different focal planes above zinc surface observed by confocal microscopy. Four planes were scanned (a) 400 μm ; (b) 800 μm ; (c) 1200 μm ; and (d) 1600 μm from the zinc floor.

Sequence of EZ Size and Galvanic Series

The Galvanic series lists metals in the order of their relative activity in a water environment. The more active (anodic) metals are highest on the list, whereas the least active (cathodic) metals are lowest. EZ size and coverage rank (see Table 1) correspond to the galvanic series rank, as shown in Table 2. The nobler the metal, the smaller the EZ, while the more active and corrosive metals present larger EZs.

Charge Separation Mechanism

Electrical potential measurements showed positive electrical potentials next to zinc, and also next to aluminum. If these are representative, then it appears that these near-metal exclusion zones are positively charged, i.e., that a high concentration of positive charge exists near reactive metal surfaces. Correspondingly, the high pH values seen beyond those near-surface zones (Fig. 8) imply a higher concentration of OH⁻ groups. A summary of the time course of charge distributions is given in Figure 13.

A question is why those charge separations occur as they do (Fig. 11). In the initial stage water molecules are neutral, while after some time charges are separated. The simplest interpretation is that water molecules are split into positive and negative moieties, the positive ones lying next to the reactive metal surfaces and the negative ones lying beyond.

However, the separation must arise from more than just proton accumulation near the reactive-metal surfaces. Protons repel one another; hence, there is no obvious reason why they might accumulate in the zone next to the metals' surface and remain there in relatively stable configuration for extended periods of time. Nor is it clear why the oppositely charged OH⁻ groups would fail to penetrate the positively charged zone.

A way of approaching an understanding is to consider what happens next to non-metallic surfaces, where exclusion zones are commonly seen adjacent to hydrophilic surfaces. In most cases the zones are charged oppositely to those seen here [9–10], although in a few instances they have similar charge distribution [10–12]. Especially in the case of the negatively charged zones, evidence shows that EZ properties differ substantially from those of water. The zone is more ordered, more stable, and has different physical and chemical properties from water [9–13]. It excludes positive charge in the same way as the exclusion zones here excludes negative charge, and the reason is that the EZ structural lattice does not permit entry. Also notable is that the zone expands in the presence of light [14].

Whether the exclusion zones found here are similar to the ones above can only be conjectured at this early stage. The main goal of the current report is to identify and detail the unexpected results, which may have important implication for metal-

surface electrochemistry, as the presence of these zones with separated charge have, to our knowledge, not been reported before. Additional studies are underway to obtain mechanistic information. It seems evident that the known ability of these reactive metals to generate negative charge could well arise out of the formation of these charge-separated

zones. Similarly, the known electropositive nature of the metals themselves could arise from the same feature — the positivity of the exclusion zone. The EZ charge-separation mechanism could be responsible for generating both features.

Table 2. Galvanic series and EZ size

Galvanic rank	4	7	27	29	44	91	92
Metals	Zinc	Aluminum	Lead	Tin	Tungsten	Gold	Platinum
EZ size (μm)	220 \pm 46.5	105 \pm 25.2	95 \pm 21.5	90 \pm 19.0	72 \pm 20.1	0	0

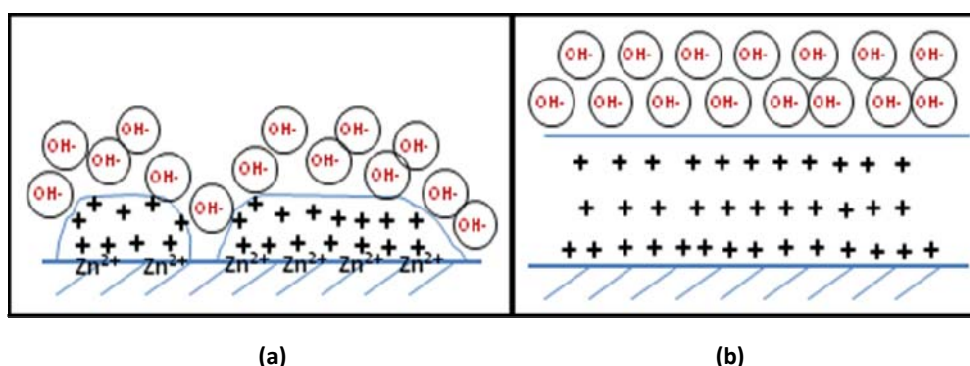


Figure 13. Diagrammatic estimate of charge distribution adjacent to zinc surface at times of (a) a few seconds; (b) 20 minutes.

Noble metals, on the other hand, showed little or no exclusion zone, and hence no charge separation. In the absence of separated charge, no reactions occur at the metal surfaces, and that is perhaps the reason that noble metals are referred to as noble. The absence of reactions also makes those them useful as electrodes. Hence, the distinction between noble and reactive metals appears to lie in whether they do or do not generate robust exclusion zones.

In some instances the exclusion zones were not uniform. They covered only a portion of the surface, and a question is why that might have been so. This feature might arise as a consequence of the charge separation itself. The metal surface, contiguous with the positively charged zone, must be positively charged. Hence, it must attract the negative OH groups. Those charged groups are ordinarily excluded by the EZ; however, if their concentration is high enough, then the charged OH groups might invade the EZ and stream toward the positive metal surface. Once that happens, building an exclusion zone might become difficult; hence the pockets would remain, between such zones of no exclusion.

An interesting feature of the results was that little oxidation occurred in zinc regions containing

exclusion zones, while considerable oxidation was seen in regions in between those exclusion zones (Figs. 11 and 12). Hence, it appears that the oxidation may be caused by currents flowing from the water to the zinc surface in regions between the pocket EZs. That might explain the spotty oxidation that is often seen.

A notable feature is that this positive-negative pair constitutes a battery, in the same way that various gels and polymers show near-surface battery features¹⁵. The presence of a “battery” next to various metal surfaces may have important implications for corrosion and also perhaps for catalysis.

5. ACKNOWLEDGEMENTS

The authors thank Jeff Magula for fabrication of the experimental chambers, Paul Wallace for training of confocal microscopy technique and the NTUF in University of Washington for supplying the confocal microscope system. This study was supported by NIH Grants (AT-002362, AR-44813

and GM-093842) and ONR Grant (N00014-05-1-0773).

6. REFERENCES

- [1] P. J. Feibelman, *Partial Dissociation of Water on Ru(0001)*, Science 295 (2002) 99–102.
- [2] D. Menzel, *Water on a Metal Surface*, Science 295 (2002) 58–59.
- [3] R. Ludwig, *Water Adsorption and Structure: How Does Water Bind to Metal Surfaces: Hydrogen Atoms Up or Hydrogen Atoms Down*. Angew. Chem. Int. Ed. 42 (2003) 3458-3460.
- [4] P. A. Thiel, T. E. Madey, *The interaction of water with solid surfaces: Fundamental aspects*, Surf. Sci. Rep. 7 (1987) 211–385.
- [5] M. A. Henderson, *The interaction of water with solid surfaces: fundamental aspects revisited*, Surf. Sci. Rep. 46 (2002) 1–308.
- [6] S. Schnur and A. Gross, *Properties of metal–water interfaces studied from first principles*, New J. Phys. 11 (2009) 125003.
- [7] Y. Gohda, S. Schnur, A. Gross, *Influence of water on elementary reaction steps in electrocatalysis*, Faraday Discuss. 140 (2008) 233.
- [8] J. M. Zheng, G. H. Pollack, *Long-range forces extending from polymer-gel surfaces*, Phys. Rev. E 68 (2003) 031408
- [9] J. M. Zheng, W. C. Chin, E. Khijniak, G. H. Pollack, *Surfaces and interfacial water: Evidence that hydrophilic surfaces have long-range impact*, Adv. Colloid Int Sci. 127 (2006) 19–27
- [10] J. M. Zheng, G. H. Pollack, *Water and the Cell: Solute exclusion and potential distribution near hydrophilic surfaces*; Springer: Netherlands, 2006, 165-174.
- [11] J. M. Zheng, A. Wexler and G. H. Pollack, *Effect of buffers on aqueous solute-exclusion zones around ion-exchange resins*, J Colloid Interface Sci. 332 (2009) 511–514.
- [12] B. H. Chai and G. H. Pollack, *Solute-free interfacial zones in polar liquids*, J. Phys. Chem. B, 114, 16,(2010) 5371–5375.
- [13] G. H. Pollack, J. Clegg, *Phase Transitions in Cell Biology: Unexpected linkage between unstirred layers, exclusion zone, and water*; Springer: New York, 2008, 143-152.
- [14] B. H. Chai, Y. Hyok and G. H. Pollack, *Spectroscopic studies of solutes in aqueous solution*, J. Phys. Chem. A, 112 (2008) 2242–2247.
- [15] B. H. Chai, J. M. Zheng, Q. Zhao and G. H. Pollack, *Effect of radiant energy on near-surface water*. J. Phys. Chem. B, 113–42 (2009) 13953–13958.
- [16] V. S. Bagotsky, *Fundamentals of Electrochemistry*; John Wiley & Sons, Inc, 2006, 379–381.



НЕОЧЕКИВАНО ПРИСУСТВО ЗОНА БЕЗ РАСТВОРЕНИХ СУПСТАНЦИ НА МЈЕСТИМА КОНТАКТА ИЗМЕЂУ МЕТАЛА И ВОДЕ

Сажетак: Зоне без растворених супстанци, назване „зоне искључења“ (зона чисте воде) обично се налазе поред хидрофилних површина у воденом раствору. Овдје смо приказали сличне зоне поред различитих метала. Највећа, широка око 200 μm , нађена је поред цинка. Остали реактивни метали, укључујући алуминијум, калај, олово и волфрам, показали су изразите али мање зоне искључења, док их код племенитих метала, као што су платина и злато, није уопште било. Мјерења електропотенцијала показала су позитивне потенцијале у оквиру зона искључења, док су мјерења pH показала обиље OH група у воденим подручјима изнад зона искључења. Установљена је подударност између величине зоне искључења и положаја дотичног метала у галванским серијама. Присуство тих зона искључења на додирној површини је неочекивано и може дати нови увид у електрохемијске процесе који се дешавају у контакту с металом.

Кључне ријечи: метали, водени раствор, оксидација, интеракција метал–вода, раздвајање набоја, зоне искључења.

